# Classification of Water Bodies Using Sentinel-2 Image and Artificial Neural Network

Zainab Adnan Mousa Safi [1*], Ehsan Ali Al-Zubaidi [2]

[1]Department of Computer Science, Faculty of Education, University of Kufa, Iraq.
E-mail: zainaba.aljbori@student.uokufa.edu.iq
[2] Department of Environmental Planning, Faculty of Physical Planning, University of Kufa, Iraq.
E-mail: Ihsana.kareem@uokufa.edu.iq

[*]Corresponding author E-mail: zainaba.aljbori@student.uokufa.edu.iq

**Abstract** This research aims to classify water bodies in Iraq using Sentinel-2A satellite images and artificial neural networks (ANNs) techniques. This satellite provides high-resolution multispectral imaging data, which helps neural networks to distinguish water from other features such as lakes, rivers, and reservoirs. An ANN model was trained using pre-labelled datasets to recognize the distinctive patterns of water. In this research, a new index called Water Body Index (WBI) is introduced to extract water bodies, which is based on the difference between six spectral bands of Sentinel-2A: blue (B), red (R), green (G), near infrared (NIR), short infrared 1 (SWIR 1), and short infrared 2 (SWIR 2). Using the neural net library in R I obtained a new linear equation that serves as the index. The new index concept had two distinct proposed versions. WBI-C (complete version). WBI-R (reduced version). The distributions of these new indices were compared with four other previously used indices: NDWI, MNDWI, MUWI-C, and MUWI-R. The results showed that WBI-C and WBI-R were more efficient in classifying water compared to vegetation, buildings, and other elements. The total average accuracy rates were: WBI-R: 99.6%, WBI-C: 99.8%, NDWI: 99.6%, MNDWI: 98.7%, MUWI-C: 98.9%, MUWI-R: 99%. As for the average Kappa Coefficient: WBI-R: 95.4%, WBI-C: 97.7%, NDWI: 85%, MNDWI: 87%, MUWI-C: 87% , MUWI-R: 89%. As for the average F-score: WBI-R: 97.7%, WBI-C: 98.9%, NDWI: 97%, MNDWI: 93.7%, MUWI-C: 93%, MUWI-R: 94%. These results show that WBI-C and WBI-R outperformed other indices in classifying water bodies with high accuracy.

*Keywords*: Water Index; Sentinel-2; ANN; Machine Learning; Remote Sensing.
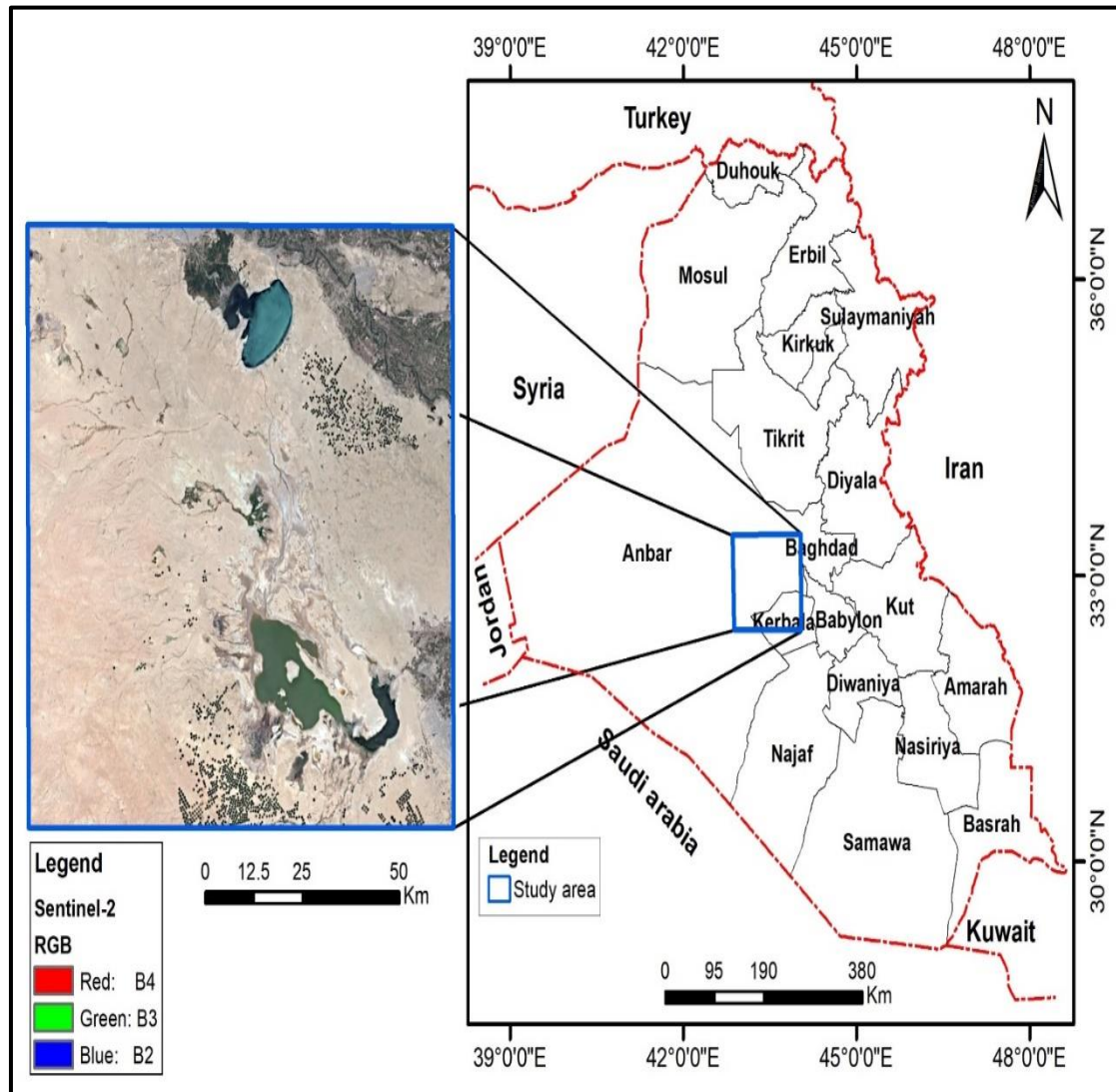
## 1. INTRODUCTION

Water bodies are natural factors that are relevant, bearing in mind their contribution towards achieving balance in the natural and fiscal structure. In addition to providing fresh water, which is crucial for supporting life forms, these water bodies also contribute to the conservation of biological diversity by offering suitable habitats to a variety of species [1, 2]. In addition to the carbon, they contain and the service they provide as thermal buffers; water bodies also play a major role in climate. In terms of economic activity, water bodies serve the military, navy, agriculture, tourism, and aquaculture by providing resources such as fish, water, and hydropower. Consequently, a system of interrelated environmental studies that would remain current with these environmental changes and provide sustainable answers to the future issues is required to understand how these entities evolve and govern them. [3]. As successor to the predecessors Spot 5 and 6 as well as Pleiades, the Sentinel-2A, The European Space Agency (ESA) initiated Sentinel-2 in 2015 to supply worldwide access to high-quality

optical remote sensing information. Due to its better spatial resolution, more spectral bands, high temporal resolution, and larger coverage area than the popular Landsat satellite, the Sentinel-2A has been shown to be useful in a variety of areas such as land cover classification, hydrology, agriculture, and soil sciences [4-9]. Water body monitoring, along with water change analysis, is facilitated by the captured high-resolution images of 10 meters and images of different spectra—near-infrared. At the same time, it is possible to monitor such events as tides or witness the presence of algae and evaluate the purity of the water with the help of Sentinel-2A images. Efficient usage of water resources and sound decision-making in areas of agriculture, economics, and environmental sciences is possible because of this data [10-12].

Machine learning is an essential and effective approach to classifying satellite images by providing quick and efficient means of considering the spectral and geographic properties of data. In other words, machine learning algorithms try to understand patterns and relevant features that allow the classification process, including but not limited to vegetation, urban structures, and water bodies [13-15]. In satellite imagery, artificial neural networks represent an effective means of classifying water features. They are capable of automatically identifying highly sophisticated patterns within a dataset; therefore, they can map large bodies of water with immense precision. In spite of certain challenges, such as the quality and the required processing of the data, the benefits of using ANNs in water body categorizations for environmental inspection, the water supply, as well as any other related aim, considerably overshadow the stated inconveniences. ANNs, especially [16], have merit in the analysis of satellite imagery and its applications in the detection and classification of water bodies and the classification of land cover [17-22]. Therefore, the focus of this research paper is to classify aquatic bodies using artificial neural networks (ANNs) based on images captured by the Sentinel-2A satellite. This goal is aimed at classifying different water body types, including lakes, rivers, swamps, and the sea, under modern satellite image processing using spectral information derived from the Sentinel-2A scenes [15, 23]. Higher resolution images are provided in the optical range, including infrared from the Sentinel-2A satellite, which greatly improves the classification. We may employ ANN to train intelligent models that take into account the differences in environmental and spectral characteristics of water bodies. All these models employ machine learning to improve the capability to predict aspects of water body environments such as pollution, water levels, and deterioration of the aquatic environment [16, 24].

## 2. STUDY AREA

Al-Razaza Lake, the second-largest lake in Iraq after Al-Thurthar Lake, is located to the northeast of Al Anbar and to the west of Karbala, as illustrated in Figure 2. The geographic coordinates of the lake are approximately [33°10′00” N, 32°20′00"N, and 43°55′00" E, 43°15′ 00” E]. This region comprises three lakes: Al-Razaza, Al-Habbaniya, and Al-Tharthar, along with Bahr Najaf. At a water elevation level of 40 meters above the mean sea level, Al-Razaza Lake has a surface area of 1810 square kilometres, with part of it in Karbala and Al-Anbar province. The water reserves in the lake approximate 26 billion m³, which are provided by the Euphrates River, Al-Habbaniya, Rashidiya, springs, and rains. The climate in the area of the lake is predominantly warm, with dry summers and wet, cold winters [25, 26]. Figure 1 shows the study area of Al-Razazza Lake.

**Figure-1** Study Area

# 3. MATERIALS AND METHODS

The methodology steps used in this paper are presented in Figure 2. The figure illustrates the R software enables the execution of ANN-based data processing after pre-processing satellite images which users download as part of the research materials.

## 3.1. MATERIALS

Sentinel-2A satellite data was used in this research to classify the water bodies of Lake Razzaza and Lake Habbaniyah, as they are important water resources in Iraq. These images obtained from the European Agency website: https://www.esa.int/ .
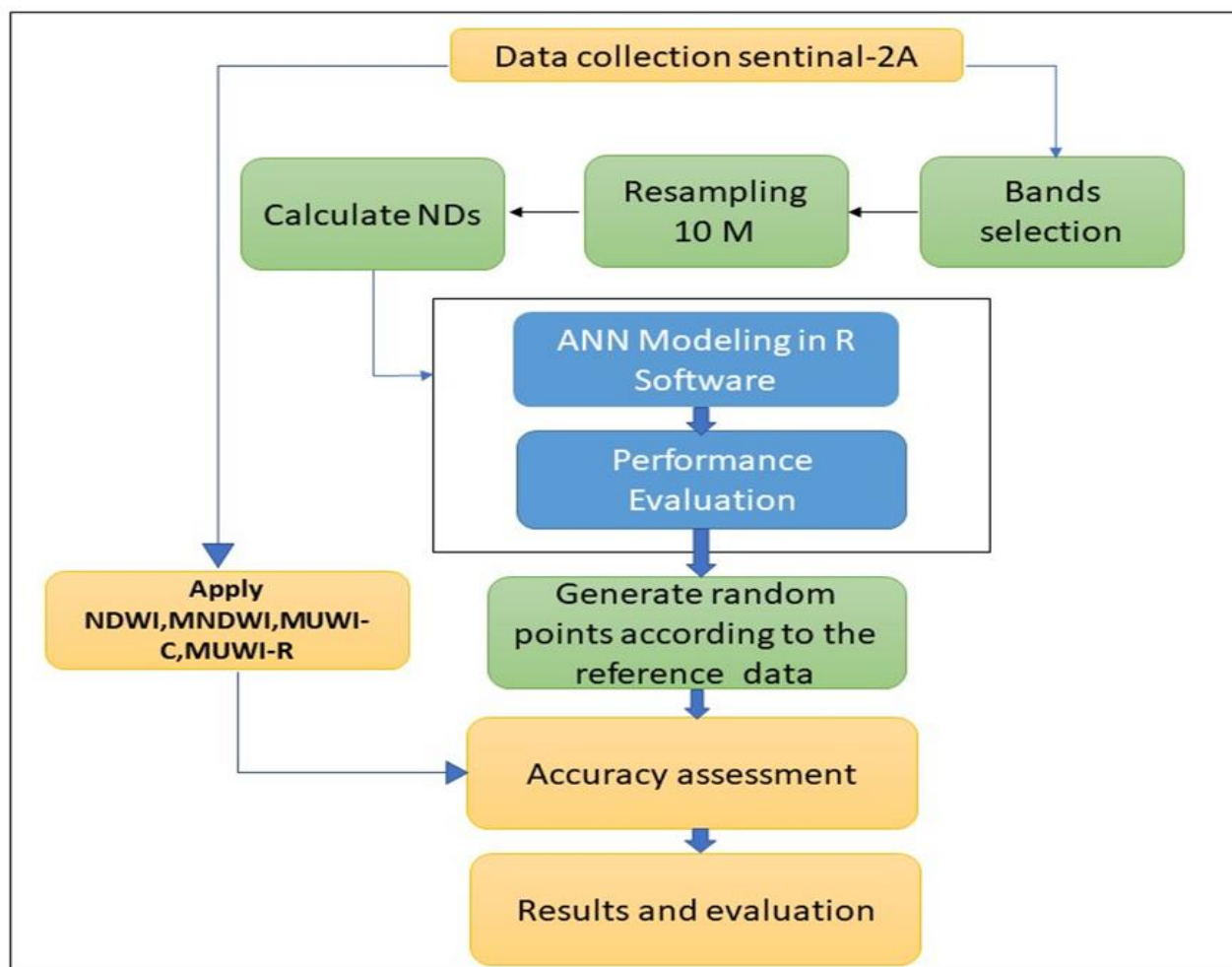


**Figure-2** Proposed Methodology

The main source of data for training and testing operations arises from Sentinel-2A satellites. Six specific bands make up the chosen selection with one visible band group and one NIR band group and two SWIR band groups. The image covers a study area of Lake Razzaza and Habbaniyah that predominantly shows aquatic and nonaquatic samples with clear polygons drawn for training the model. The RGB configuration utilizes the Sentinel-2A bands. There, red stands for near-infrared (NIR), green stands for red, while blue stands for green. Blue polygons represent the water samples, making it easy to distinguish water bodies like lakes and rivers. We can clearly distinguish the main lake from the other land masses in the middle of the image. Orange polygons depict non-aquatic habitats that include, as shown in figure 3, dryland vegetation and the urban environment. These areas are distributed evenly in the study area and are referred to as training samples for nonaquatic area classification. The near-infrared range emphasizes the vegetation in this image, making it easier to distinguish it from water and bare ground. The image includes training polygons for supervised classification: blue polygons for water samples and orange polygons for non-water samples. The placement of these polygons is intentional to account for individual

landscape heterogeneities. The aim and purpose of this categorization procedure is to correctly differentiate between water areas, for example, lakes and tributaries, and non-water zones like drips and vegetation regions. The training polygons thus assist the classification algorithms to capture the variation in the land cover attributes.
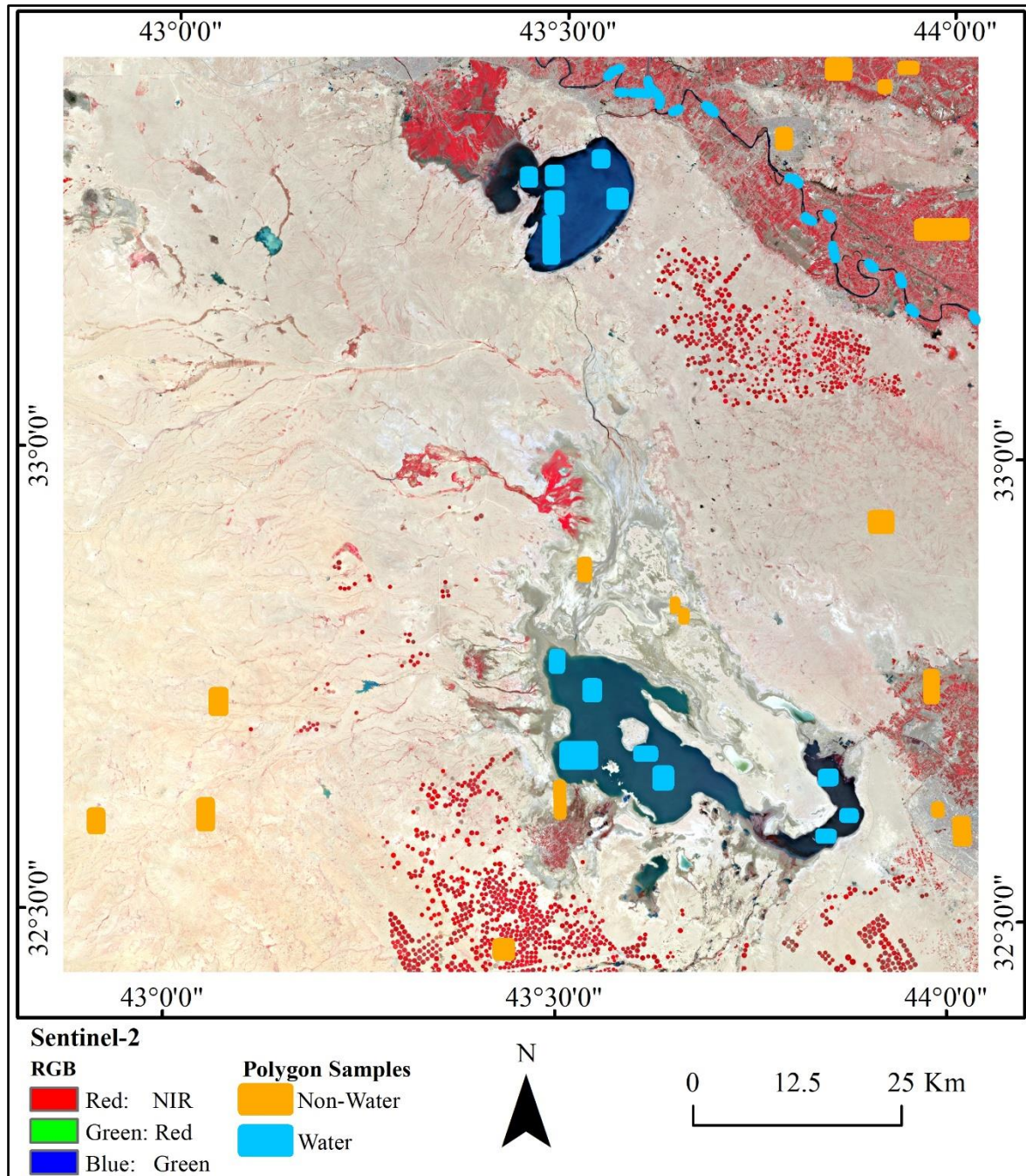


**Figure-3** Training Samples for Water Classification.

After selecting the six bands for (780236) pixels for the training process and after resampling so that all bands are 10-meter bands, the normalized difference index was calculated. It is crucial for satellite

image classification since it enhances the model's prediction and classification accuracy and efficiency, expedites the learning process, and makes the models function more effectively, also to measure the variance between each band and the other, as in previous studies [27, 28], according to the following equation:

$$NDs = \frac{Bandi - Bandj}{Bandi + Bandj} \qquad (1)$$

Where ND is normalized difference, Band i and Band j are number of bands. After calculating the normalized difference index, 15 bands are obtained, including the six previously selected bands. The materials used in this research include the ArcGIS Map tool and the website of the European Agency of the Sentinel-2A satellite, where the images of the study area were downloaded: Lake Razzaza. The GIS tool, as a mechanism applied to all systems, serves to interrogate and process all forms of image dimensions and to calculate and assess the values of resolution. In this research, we utilized the following GIS tools for display and image processing: The resample tool was used to set the number of required bands again, and under image settings, the highest permissible resolution was set to 10 meters for all the selected bands, apart from the Reclassify tool to reclassify the image to be one band: 1 for water and 0 for others.

## 3.2 METHODS

In fields like machine learning and remote monitoring, artificial neural networks (ANNs) are crucial instruments for data classification. Artificial neural networks (ANNs) assess and categorize large volumes of complex data effectively. Using artificial neurons in multiple layers, ANNs mimic the way the brain works and can help to solve complex patterns and relationships in data. As they are trained using the input data and adapt the weight between the neurons to get the best categorization done, their highest advantage is the ability to enhance classification performance. There is also a possibility of analyzing non-linear data—something that would be extremely difficult to analyze with the help of normal techniques since this is made possible by neural networks. Unlike other methods such as Decision Trees or Regression algorithms, artificial Neural Networks (ANNs) have shown high efficiency in practices such as satellite image classification and even environmental prediction, as suggested in He et al. (2019) and LeCun et al. (2015).

### 3.2.1 Water Bodies Indices

Mathematical expression for the water body index (WBI) is:

$$WBI = \sum a_i \, p_i \, -b \qquad (2)$$

where ai refers to the weights obtained during training of the artificial neural network (ANN) model, pi represents the spectral bands used as input features, and b refers to the bias derived from the ANN model. The NDWI offers contemporary upgrades for remote sensing image water element identification while assessing turbidity strength and water extent mapping [29].

$$NDWI = \frac{B3 - B8}{B3 + B8} \qquad (3)$$

NDWI uses the NIR band's strong water information about mine water absorption from images, the low light condition creates open views that highlight both water sources and eliminate plant life. However, it ignores buildings and soil features, leading to confusion with soil and building information. Urban water bodies with more building shadows have poor results [25].

The MNDWI serves as a modified version of normalized difference water index (NDWI) through its substitution of middle infrared band instead of the near-infrared band, enhancing open water features whilst suppressing constructed-up land noise and flora. The MNDWI calculation includes parameters such

as contrast value, mean of foreground target (water), and mean of background target (non-water feature) [30].

$$MNDWI = \frac{B3 - B5}{B3 + B5} \qquad (4)$$

Where MNDWI uses shortwave infrared (SWIR) bands of satellite images is B5, as well as green bands as B3. MUWI-C is a version of the Multi-Spectral Water Index (MuWI) that consists of multiple terms derived from normalized differences in Sentinel-2A bands and is designed to improve water mapping accuracy. MUWI-C is designed to improve the spatial resolution and accuracy of water mapping on Sentinel-2A by utilizing specific bands and refined terms. MUWI-C utilizes bands from ND23, ND38, and ND312 for correct water mapping on Sentinel-2A [31].

MuWI-C = (−16.4ND2,3 − 6.9ND2,4 − 8.2ND2,8 − 8.8ND2,11 +9.6ND2,12 + 10.8ND3,8 + 6.1ND3,11 + 13.6ND3,12 −0.28ND4,8 − 3.9ND4,11 − 2.1ND4,12 − 5.3ND8,11−5.3ND8,12 − 5.3ND11,12 - 0.33) (3)

The Sentinel-2A band (I) and band (J) normalized difference is designated as ND (I, J). Standard water mapping may not require all terms contained in MuWI-C because its current term count is excessive. Four essential terms have been added to MuWI-C with large integer coefficients to create modified version. The MUWI-R has been updated to make accurate water mapping on Sentinel-2A images. It does this by reducing commission and omission errors, such as shadow and sun glint misclassifications. MUWI-R is a refined version of MuWI that enhances the accuracy and backbone of water mapping on Sentinel-2A imagery [31].

MuWI-R = -4"ND23"+2"ND38"+2"ND312"-"ND311" (6)

The four highest weight expressions in MuWI-C consist of ND (2,3) and ND (3,12) as well as ND (3,8) with ND (3,11) designated for high-albedo aquatic pixels. We skip discussing the standard time limits of MuWI-R while presenting Table 1 with this summary of indicators.

**Table 1-** Water indices

| water Index | Equation | Threshold value |
|---|---|---|
| NDWI | (Bgreen-Bnir)/ (Bgreen+Bnir) | 0.2 |
| MNDWI | (BgreenBswir)/(Bgreen+Bswir) | 0.3 |
| MUWI-R | -4"ND23"+2"ND38"+2"ND312"-"ND311" | -1.7 |
| MUWI-C | −16.4ND23−6.9ND24−8.2ND28−8.8ND211 +9.6ND212+10.8ND38+6.1ND311+13.6ND312−0.28ND48−3.9ND41 1− 2.1ND412 −5.3ND811−5.3ND812− 5.3ND1112 − 0.33 | 0.33 |

### 3.2.2 Accuracy assessment

All the classifiers were evaluated for classification accuracy and Cohen's kappa coefficient using ArcGIS software by analysing five random point sets which extended from 1000 up to 5000 points. Obtain the reference class type information and ANN result class type information along with class type information from previous studies (Table 1) from the images. All accuracy assessment parameters contained a confusion matrix in combination with overall accuracy (OA) and Cohen's kappa coefficient (K) and F-score values. The errors originated from correct pixel identifications according to data in Table 2.

**Table 2-** Confusion Matrix

|  |  | Class prediction | |
|---|---|---|---|
|  |  | +1 | -1 |
| **Existing** | **+1** | TP | FN |
| **class** | **-1** | FP | TN |

The correct diagnoses label both TP and TN as True. A detection of +1 as positive during an operation which produced -1 results in a false positive (FP). A negative test reading points to a false negative rate (FN) because the actual outcome was positive [22]. The Cohen's Kappa value appears within the two-dimensional confusion matrix used by researchers for statistical classification work [27]. The calculations utilize this formula for determining these measurements: The OA and Kappa.

$$Overall\ Accuracy = \frac{TP+TN}{TP+TN+FP+FN} \qquad (7)$$

$$kappa = \frac{Po+Pe}{1-Pe} \qquad (8)$$

$$Po = \frac{TP+TN}{TP+TN+FP+FN} \qquad (9)$$

$$Pe = P(+1) + P(-1) \qquad (10)$$

$$P(+1) = \frac{TP+FN}{TP+TN+FP+FN} * \frac{TP+FP}{TP+TN+FP+FN} \qquad (11)$$

$$P(-1) = \frac{FP+TN}{TP+TN+FP+FN} * \frac{TN+FN}{TP+TN+FP+FN} \qquad (12)$$

A F-score evaluation of classification results ensures accuracy outcomes. The F-score computes as the harmonic mean value between UA and PA values. Equations have been used to derive all three figures which comprise the PA, UA, and F [28].

$$PA = \frac{TP}{TP+FN} \qquad (13)$$

$$UA = \frac{TP}{TP+FP} \qquad (14)$$

$$F\text{-}score = \frac{2*PA*UA}{PA+UA} \qquad (15)$$

## 4. RESULTS AND DISCUSSION

This section presents the results of water body classification using the proposed Water Body Index (WBI) and compares its performance with existing indices. The classification accuracy, Kappa coefficient, and F-score are analyzed to evaluate the effectiveness of WBI-C and WBI-R in distinguishing water bodies from other land cover types. Additionally, a comparative assessment is conducted with the widely used NDWI, MNDWI, MUWI-C, and MUWI-R indices. The results highlight the strengths of the proposed indices and their applicability for accurate water body extraction in Iraq.

*4.1 RESULTS*

The index initially incorporates training features as the first term of the product contains 15 NDs. An easy-to-use formula emerges from the removal of unimportant weight terms during the second development stage where necessary non-core requirements in system functionality are identified. All WBI index versions can be found in the following Table 3.

**Table 3**. Two Versions of The WBI Index

| Index | | Formula | Threshold |
|-------|--|---------|-----------|
| BI-C | ١ | -165* "ND23"+ 8*"ND24"+18*"ND28"+6*"ND211"-30*"ND212"+ 194*"ND34"+ 187*"ND38"+ 70*"ND311"+ 43*"ND312"+ 25*"ND48" -5*"ND411" -18*"ND412" -15*"ND811" -45*"ND812" 165*"ND1112" | ٢٩,١١٥ |
| BI-R | ١ | 298*"ND34"+"ND38" *313-23*"ND312" | -٢١,٦٨٤ |

The available number of ND between bands determines the value of i and j in this expression. The two forms of weight buffeting intensity formula (WBI-C and WBI-R) were both applied to compare their performances against previous aquatic indexes. Bearing the core elements of this index proposal stands WBI-R but WBI-C demonstrates the entire format of the proposed index with all its features. The format of WBI-R adapts better to entire scenes and produces more accurate satellite image categorization compared to the WBI-C index.

### 4.1.1 Quantitative Assessment

WBI index on 10 m resolution Sentinel-2A satellite images of Razzaza Lake and compared it with five indices from previous studies: NDWI, MNDWI, MUWI-C, and MUWI-R. Based on the results obtained, WBI-R gave excellent results compared to the other indices in terms of identifying the boundaries of water bodies. Table 4 compares the accuracy of NDWI, MNDWI, MUWI-R, MUWI-C, WBI-C, and WBI-R The researcher employed three evaluation metrics including both accuracy measures and kappa coefficient and F-score.

**Table -4**. Summary of the accuracy of WBI and four water index methods

| Metrics | MUWI-R | MUWI-C | MNDWI | NDWI | WBI-C | WBI-R |
|---------|--------|--------|-------|------|-------|-------|
| Overall accuracy (OA) | 99 | ٩٨,٩ | ٩٨,٧ | ٩٩,٦ | ٩٩,٨ | **99.6** |
| Kappa Coefficient | ٨٩ | ٨٧ | ٨٥ | ٩٥,٤ | ٩٧,٧ | ٩٥,٣ |
| F-score | ٩٤ | ٩٣,٧ | ٩٣ | ٩٧,٧ | ٩٨,٩ | ٩٨ |

The WBI-C model detects 99.8% of open water conditions while the WBI-R model detects 99.6%. Both versions of WBI produce statistically better classification performance than the other four water indices. The reference dataset reveals highest agreement between WBI-C combined with WBI-R according to kappa coefficient results. WBI-C performs best when classifying water compared to WBI-R while WBI produces better results than NDWI, MNDWI, MUWI-C and MUWI-R based on Figure 4 that presents statistical data about these indices for the performance measures used.
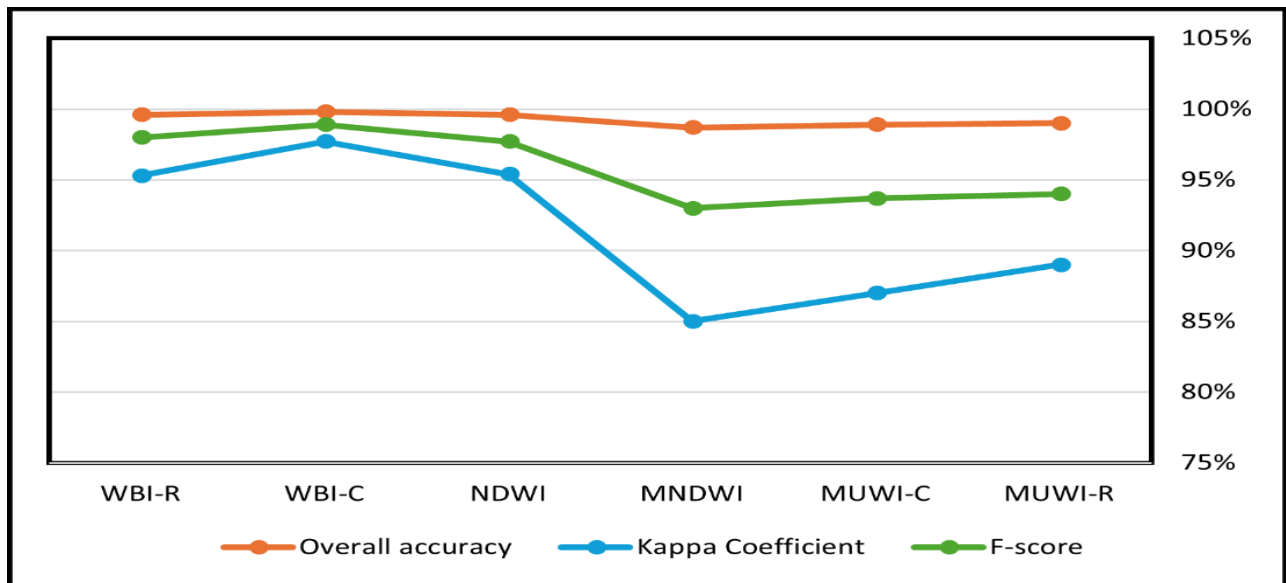
**Figure -4** Indicators Statistics

Table 4 also shows the results obtained from the six water indices: NDWI, MNDWI, MUWI-R, MUEI-C, and WBI of both Lake Razzaza and Lake Habbaniyah at a 10m resolution. When comparing across the indicators, it can be seen that the WBI indicators are more suitable for identifying water boundaries. They help in defining thresholds and enable pixel values to be categorized as wet or non-water depending on the determined threshold values. In the process of defining water bodies, threshold values play a crucial role as they facilitate the interpretation of index values. It also has the advantage of sorting conditions that may exist alongside the water quality it assists in management decisions. It helps the ease and enables the distinction between the various concentrations of pollutants, turbidity, and other compounds and assists the authorities in taking necessary actions. If the index value turns out to be a positive number, then it is zeroed to water, and if the index turns out to be a negative number, it is zeroed to non-water, but water indices usually contain zero as the break point or threshold.

*4.1.2 Qualitative Analysis*

The classification results showed that the WBI provided the highest level of accuracy in representing water areas within the study area. The WBI maps had a clean color wash-off, which separated the water from the phenomenal and the phenomenal from the water, and hence there was high accuracy in the definition of water body limits as shown in Figure 5. Hence, the maps produced by other indices (NDWI, MNDWI, and MUWI) introduced larger overlaps in the classes of land, and thus, the identification of water zones distorted, especially in the areas being overgrown with vegetation or having rugged relief. This difference in performance can be attributed to the relative variability of other indices depending on changes in vegetation cover and other surfaces, which in turn influences the reflectivity value at different wavelengths.

Figure 6 shows a set of classified maps obtained using different water identification indices at three sites (Site 1, Site 2, Site 3) and a reference site. The wide-area water indices (WBI), (NDWI), the urban water index (MNDWI), and two forms of the multispectral water index (MuWI) (MuWI-C and MuWI-R) were used. The aim of these maps was to evaluate the performance of each index in accurately identifying water and compare it with the reference site. To verify the accuracy of the classification results, a comparison was made between the classified images and the reference map. The reference map, derived from high-resolution images and real data, served as a benchmark for evaluating the performance of the different water indices.

The reference map clearly identifies the water bodies within the study area. When comparing the classified images to the reference, it is clear that the WBIs index gave the most accurate results. This index effectively distinguished between water and non-water areas, with minimal false positives or false negatives. The NDWI index also performed reasonably well, although it showed some overestimation of water areas in certain areas. On the other hand, the MNDWIs and MUWIs indices showed the lowest accuracy, especially in areas with complex land cover. Locations with abnormally high reflectance in Figure 6 are likely the result of the sun blink phenomenon. The MUWIs map incorrectly classifies a bright area because sites 1 and 2 show non-water identification possibly because of algorithm performance or noise. Water areas within the lower part of Figure 6 received wrong classifications utilizing MNDWI and NDWI methodologies. Solar flash pollution allows WBI-C and WBI-R to locate and identify water pixels in different areas.
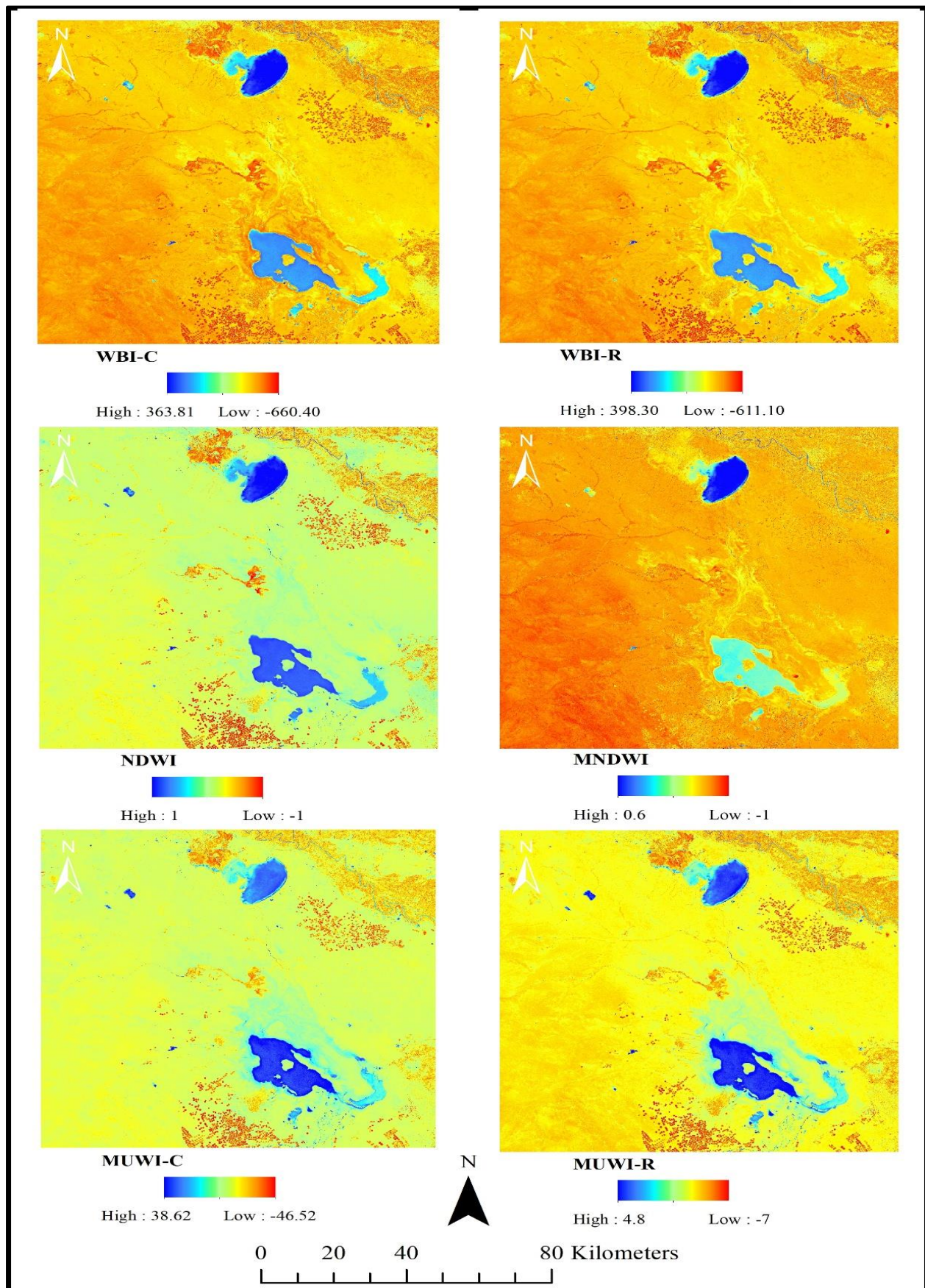
**Figure 5.** Water Spectral Indices (NDWI, MNDWI, MUWI-C, MUWI-R, WBI-C, WBI-R
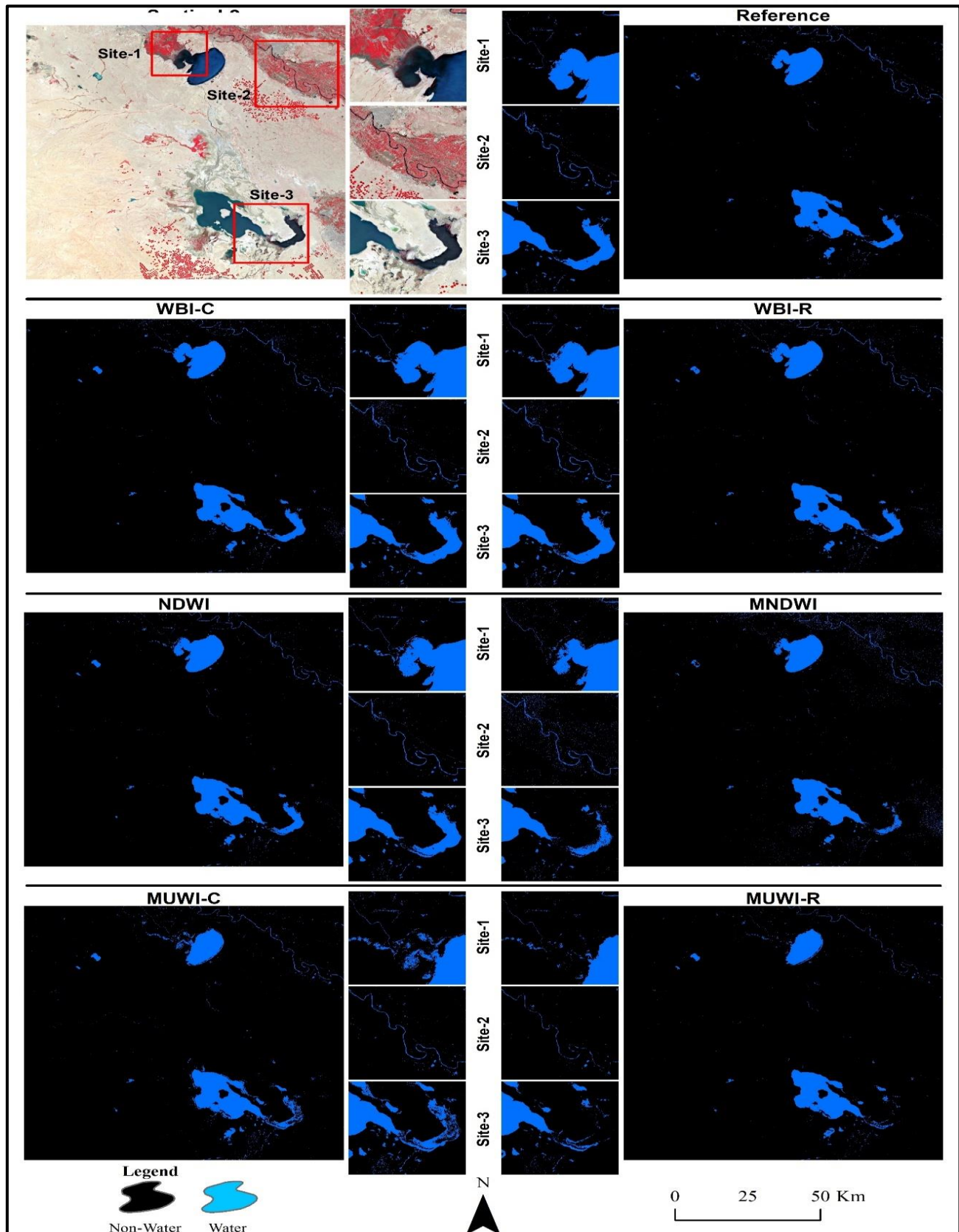
**Figure 6**. Binary image of water spectral indices (NDWI, MNDWI, MUWI-C, MUWI-R, WBI-C, WBI-R

*4.2 DISCUSSION*

Spatial resolution plays a vital role in enhancing the accuracy of water mapping, making it a significant factor in the improvements observed in the Water Body Index (WBI). Despite the underutilization of Sentinel-2A's native 10-meter resolution, the variation in spatial resolution among its different bands often forces traditional water indices to rely on a 20M resolution for water maps. Previous studies have explored band-optimization techniques to achieve 10-meter resolution water maps; however, these methods require intensive computational resources, making them time-consuming, particularly when dealing with extensive areas.

Conversely, the Normalized Water Index (NDWI) utilizes two 10M bands from Sentinel-2A but encounters issues such as incorrect water classification leading to commission errors. In contrast, the development of WBI incorporates all three 10-meter bands from Sentinel-2A as key inputs. The training process of the artificial neural network (ANN) algorithm significantly enhances the weights of these bands, even with the inclusion of 20M resolution bands. By carefully selecting the bands to use in WBI and applying machine learning techniques, we can create water maps with a 10-meter resolution without the need for extra band optimization. This guarantees that water mapping effectively uses the crucial data from the 10-meter bands.

## 5. CONCLUSIONS

This study introduced a new automated water index (WBI). Sentinel-2A MSI images yielded water maps with a native resolution of 10 m. One important methodological advantage of this work is the application of the ANN machine-learning technology to provide a unique and objective index. When compared to the water index methods developed using Landsat data, the proposed WBI method yielded water maps with a better spatial resolution (10 m). The effective use of Sentinel-2A's built-in 10-m spectral bands is responsible for this improvement, which also includes a noticeable drop in misclassifications brought on by sun glint and shadows. However, all indices remain challenging in regions with a mixture of macrophytes or algae. Improved simplicity and accuracy are the features of the updated version of the WBI-R. With the growing amount of Sentinel-2A imagery, this suggested method could simplify precise water mapping and pave the way for more extensive use in the future.

## REFERENCES

[1] Sheffield, J., et al., Satellite Remote Sensing for Water Resources Management: Potential for Supporting Sustainable Development in Data-Poor Regions. Water Resources Research. 54(12): p. 9724-9758 .2018.

[2] Al-Janabi, A., E.A. Kareem, and R.H.A. Al Sagheer, Encapsulation of semantic description with syntactic components for the Arabic language. Indonesian Journal of Electrical Engineering and Computer Science, 2021. 22.(٢)

[3] Pettorelli, N., K. Safi, and W. Turner, Satellite remote sensing, biodiversity research and conservation of the future. Philos Trans R Soc Lond B Biol Sci. 369(1643): p. 20130190. 2014.

[4] Sadeghi, M., et al., The optical trapezoid model: A novel approach to remote sensing of soil moisture applied to Sentinel-2A and Landsat-8 observations. 198: p. 52-68.2017.

[5] Brezonik, P.L., et al., Factors affecting the measurement of CDOM by remote sensing of optically complex inland waters. Remote Sensing of Environment. 157: p. 199-215.2015.

[6] Gómez, C., J.C. White, and M.A. Wulder, Optical remotely sensed time series data for land cover classification: A review. ISPRS Journal of Photogrammetry and Remote Sensing. 116: p. 55-72.2016.

[7] Kaplan, G. and U. Avdan, Object-based water body extraction model using Sentinel-2A -2 satellite imagery. European Journal of Remote Sensing. 50(1): p. 137-143.2017.

[8] Pahlevan, N., et al., Sentinel-2A MultiSpectral Instrument (MSI) data processing for aquatic science applications: Demonstrations and validations. Remote sensing of environment. 201: p. 47-56. 2017.

[9] Puliti, S., et al., Combining UAV and Sentinel-2A auxiliary data for forest growing stock volume estimation through hierarchical model-based inference. Remote Sensing of Environment. 204: p. 485-497. 2018.

[10] Al-Zubaidi, A.P.E.A., F. Rabee, and A.H. Al-Sulttani, Classification of Large-Scale Datasets of Landsat-8 Satellite Image Based on LIBLINEAR Library. Al-Salam Journal for Engineering and Technology. 1(2): p. 9-17. 2022.

[11] Jiang, W., et al., A New Index for Identifying Water Body from Sentinel-2A -2 Satellite Remote Sensing Imagery. ISPRS Annals of the Photogrammetry, Remote Sensing and Spatial Information Sciences. V-3-2020: p. 33-38. 2020.

[12] Feng, Q., J. Liu, and J. Gong, UAV Remote Sensing for Urban Vegetation Mapping Using Random Forest and Texture Analysis. Remote Sensing. 7(1): p. 1074-1094. 2015.

[13] Camps-Valls, G. and L. Bruzzone, Kernel-based methods for hyperspectral image classification. IEEE Transactions on Geoscience and Remote Sensing. 43(6): p. 1351-1362. 2005.

[14] Bai, T., et al., Cloud Detection for High-Resolution Satellite Imagery Using Machine Learning and Multi-Feature Fusion. Remote Sensing. 8.(٩). 2016.

[15] Al-Zubaidi, E.A., F. Rabee, and A.H. Al-Sulttani, Calculating Spectral Index Based on Linear SVM Methods for Landsat OLI: Baiji Sand Dunes a Case Study, Iraq. International Journal of Computing and Digital Systems. 13(1): p. 1-15. 2023.

[16] Rasheed, M.U. and S.A. Mahmood, A framework based on deep neural network (DNN) for land use land cover (LULC) and rice crop classification without using survey data. Climate Dynamics. 61(11-12): p. 5629-5652. 2023.

[17] Civco, D.L.J.I.j.o.g.i.s., Artificial neural networks for land-cover classification and mapping. 7(2): p. 173-186. 1993.

[18] Jensen, J.R. and K. Lulla, Introductory digital image processing: a remote sensing perspective. 1987.

[19] Chebud, Y., et al., Water quality monitoring using remote sensing and an artificial neural network.. 223: p. 4875-4887. 2012.

[20] Nasir, N., et al., Water quality classification using machine learning algorithms.48: p. 102920. 2022

[21] Skakun, S.J.C. and Informatics, A neural network approach to flood mapping using satellite imagery. 29(6): p. 1013-1024. 2010.

[22] Al-Zubaidi, E.A., A.H. Al-Sulttani, and F. Rabee, Sand Dunes Spectral Index Determination Using Machine Learning Model: Case study of Baiji Sand Dunes Field Northern Iraq. Iraqi Geological Journal. 55(1F): p. 102-121. 2022.

[23] Mueller, N., et al., Water observations from space: Mapping surface water from 25 years of Landsat imagery across Australia. Remote Sensing of Environment. 174: p. 341-352. 2016.

[24] Hafeez, S., et al., Evaluating Landsat-8 and Sentinel-2A -2 Data Consistency for High Spatiotemporal Inland and Coastal Water Quality Monitoring. 14(13): p. 3155. 2022.

[25] Liu, H., et al., A Comparison of Different Water Indices and Band Downscaling Methods for Water Bodies Mapping from Sentinel-2A -2 Imagery at 10-M Resolution. Water. 14.(١٧). 2022

[26] Al-Ansari, N.A., Management of Water Resources in Iraq: Perspectives and Prognoses. Engineering. 05(08): p. 667-684. 2013.

[27] Chicco, D., M.J. Warrens, and G.J.P.c.s. Jurman, The coefficient of determination R-squared is more informative than SMAPE, MAE, MAPE, MSE and RMSE in regression analysis evaluation. 7 :p. e623  2021.

[28] Xiao, W., et al., Anatomy of composition and nature of plate convergence: Insights for alternative thoughts for terminal India-Eurasia collision. 60: p. 1015-1039. 2017.

[29] McFeeters, S.K., The use of the Normalized Difference Water Index (NDWI) in the delineation of open water features. International Journal of Remote Sensing. 17(7): p. 1425-1432. 2007.

[30] Xu, H., Modification of normalized difference water index (NDWI) to enhance open water features in remotely sensed imagery. International Journal of Remote Sensing. 27(14): p. 3025-3033.2007.

[31] Wang, Z., et al., Multi-Spectral Water Index (MuWI): A Native 10-m Multi-Spectral Water Index for Accurate Water Mapping on Sentinel-2A -2. Remote Sensing, 2018. 10(10).